

Elliptic Polarization of Balmer Radiation from Low-Energy Grazing-Incidence Collisions of Hydrogen Ions on Surfaces

N. H. Tolk, J. C. Tully, and J. S. Kraus
Bell Laboratories, Murray Hill, New Jersey 07974

and

W. Heiland
Max-Planck-Institut für Plasmaphysik, EURATOM Association, 8046 Garching, München, Germany

and

S. H. Neff
Earlham College, Richmond, Indiana 47347
 (Received 30 May 1978)

Pronounced elliptic polarization has been observed in Balmer radiation following low-energy grazing-incidence collisions of H^- , H^+ , H_2^+ , and H_3^+ on a clean lead surface maintained under ultrahigh vacuum. The polarization, shown to arise predominantly from p states, is found to depend only on velocity, not on the charge or molecular species of the incoming projectile. A two-step surface-interaction model is presented based on anisotropic near-resonant electron pickup followed by quantum mechanical phase evolution.

We have observed strong elliptic polarization arising from the p -state component of Balmer radiation emitted following low-energy (0.6 to 10 keV/nucleon) grazing-incidence collisions of beams of H^- , H^+ , H_2^+ , and H_3^+ ions on various sputter-cleaned polycrystalline metal surfaces, in particular Pb, maintained under ultrahigh vacuum (10^{-10} Torr). Andrä and co-workers^{1,2} and Berry *et al.*³ have observed elliptic polarization from grazing-incidence experiments at higher energies (40 keV to 2.5 MeV). The measurements reported here are the first to be performed at low energies, with a variety of molecular hydrogen ions, and in a clean environment. Our observations lead us to suggest a new physical model involving a direct anisotropic electron-pickup mechanism with subsequent modification of polarization due to electrostatic interaction of the atom with the surface.

The experimental apparatus consists of an ion source, electrostatic focus lenses, a Wien velocity filter, and an ultrahigh-vacuum chamber capable of sustaining an ambient pressure of 10^{-10} Torr. Mass-separated atomic and molecular ion beams are produced in the energy range from 50 eV to 10 keV. Polarization data are acquired with a Polaroid HN-38 polarizer, a depolarizer which removes spectrometer polarization bias, and a retardation plate with quarter-wave retardation at 656.3 nm. Single-photon counting techniques are used to detect and process photons emitted normal to the plane defined by the incoming beam and surface normal (out of the page in Fig. 1).

The optical radiation observed in this experiment arises from the decay of $3s$, $3p$, and $3d$ states of hydrogen excited by grazing-incidence collisions of H^- , H^+ , H_2^+ , or H_3^+ on an approximately 2-mm-wide Pb surface as shown in Fig. 1. Ta, Cu, Mo, and C targets were also used; however, the Pb target was found to produce the highest light intensity as well as the highest degree of polarization. Relatively small amounts of linear polarization were observed. In terms of normalized Stokes parameters,² typical values were $M/I \approx 0.01$ and $C/I \approx -0.10$. Consequently, the major axis of elliptic polarization was observed to be approximately at 45° from the x axis in Fig. 1 in the clockwise direction. The greatest contribution to the fractional polarization in this experiment arose from the normalized Stokes parameter expressing circular po-

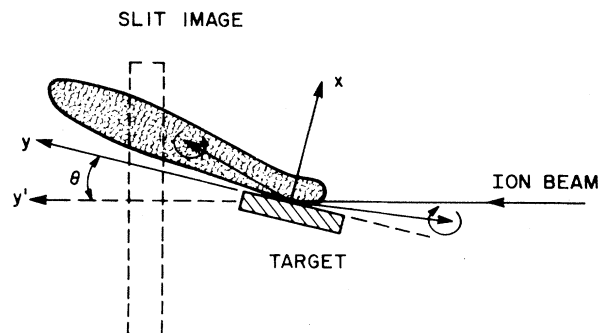


FIG. 1. Schematic representation of experimental configuration.

larization given by

$$S/I = (I_{RH} - I_{LH}) / (I_{RH} + I_{LH}), \quad (1)$$

where I_{LH} and I_{RH} are the intensities of left and right circularly polarized light, respectively. Strong left-hand polarization with values of S/I of the order of -0.50 were observed. These measurements were found to be only very weakly dependent on grazing incidence angle θ (see Fig. 1) in the range of measurement, $\theta = 1$ to 7 deg. Introduction of a small partial pressure of oxygen (10^{-7} Torr) caused severe reduction in the degree of circular polarization, thereby underscoring the importance of clean surfaces.

As shown in Fig. 1, measurements as a function of the position y' of the detector slit along the beam direction were acquired by sampling a region of observation defined by one-to-one image of the monochromator entrance slit of dimensions 2 cm by 0.2 cm. A typical measurement of intensity and degree of circular polarization S/I as a function of y' is shown in Fig. 2 for the case of 10-keV H_2^+ grazing-incidence (6°) collision on a 2-mm-wide Pb target centered at $y' = 0$. Note that S/I changes sign for large negative values of y' , suggesting that ions which are scattered at large angles, $> 90^\circ$, have orientation opposite to those scattered at small glancing angles. Note also that $|S/I|$ decreases markedly as a function

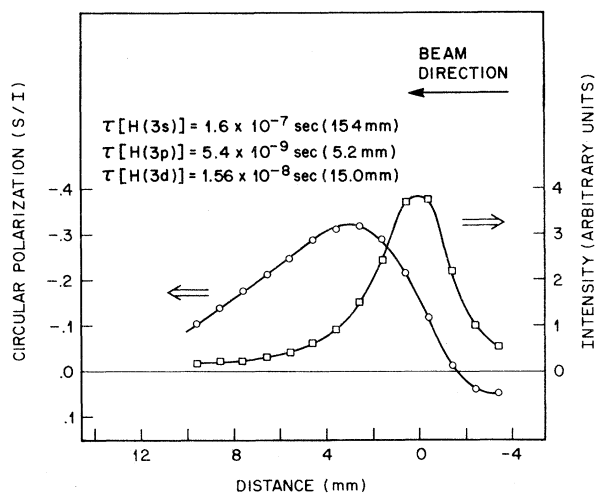


FIG. 2. Radiation intensity (boxes) and circular polarization S/I (open circles) of H_α radiation shown as a function of distance along the beam for 10-keV H_2^+ on Pb at a 6° grazing angle. The target region is 2 mm long in the beam direction centered at 0 mm. The acceptance width for radiation detection, determined by the slit width, is 2 mm.

of y' downstream from the target, behavior not observed in previous measurements.¹⁻⁴ Since projectiles are not slowed appreciably during grazing collisions, we can relate directly this decay with distance to a decay with time. From Fig. 2 we extract a decay of circular polarization with time of $\sim 5 \times 10^{-9}$ sec. Roughly the same decay time was obtained for a variety of incident energies and with H^+ and H_3^+ as well, and it corresponds very closely to the 5.4-nsec lifetime of the $3p$ state of H. We deduce from this that while all three components, $3s$, $3p$, and $3d$, contribute in undetermined ratios to the total intensity, the principal, if not exclusive, contributor to circularly polarized radiation is the $3p$ state.

The energy dependence of circular polarization S/I in H_α from H^+ , H_2^+ , and H_3^+ grazing-incidence collisions on Pb is plotted in Fig. 3(a). Figure 3(b) portrays the same data as in Fig. 3(a) but plotted as a function of energy per nucleon show-

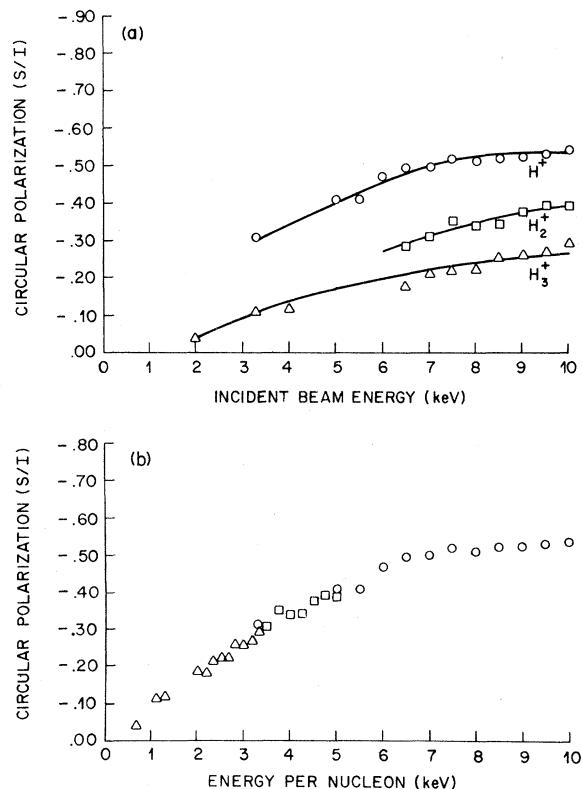


FIG. 3. (a) Measurements of circular polarization S/I for beams of H^+ , H_2^+ , and H_3^+ incident at 6° grazing angle on lead as a function of beam energy. (b) Same data as in (a) plotted as a function of energy per nucleon.

ing that the resulting $H^*(3p)$ "loses memory" as to whether the projectile began as part of a H^+ , H_2^+ , or H_3^+ complex and depends only on its initial velocity. Similar results were also obtained for H^- projectiles.

We present a model to explain the characteristics of the observed polarization which separates the mechanism into two parts: (a) the initial production of anisotropic states, and (b) their subsequent evolution due to a surface electrostatic interaction.⁴ To illustrate part (b), consider an atom prepared in a pure p ($m_l = -1$) state (pure orientation) at a distance x_0 from the surface with constant velocity v_\perp , experiencing only static interaction normal to the surface. In our viewing geometry the normalized Stokes parameters would be given by

$$\begin{aligned} S/I &= -\cos(\Delta/\hbar v_\perp), \quad M/I = 0, \\ C/I &= \sin(\Delta/\hbar v_\perp), \end{aligned} \quad (2)$$

where

$$\Delta = \int_{x_0}^{\infty} [E_{p_x}(x) - E_{p_y}(x)] dx, \quad (3)$$

v_\perp is the component of velocity perpendicular to the surface, and $E_{p_x}(x)$ and $E_{p_y}(x)$ are the energies of the p_x and p_y states at a distance x from the surface. Thus if the system begins in a pure orientation state, the major axis of elliptic polarization must be at $\pm 45^\circ$ to the surface normal, consistent with our experimental observations. At velocities $v_\perp \ll \hbar^{-1}\Delta$ polarization effects will be washed out. Since they are not washed out in our low-energy experiments [v_\perp ranging from $(3.5$ to $14) \times 10^6$ cm/sec, corresponding to energies 6.5–110 eV] Δ must be small. S/I , as shown in Fig. 3, increases with increasing energy, i.e., increasing v_\perp . In addition, M/I is nearly zero and C/I (not shown) decreases with increasing v_\perp , in qualitative agreement with Eq. (2). By fitting

$$\begin{aligned} &\langle \varphi_s | \tilde{V}(x) | \varphi_H \rangle \\ &\sim \langle \exp(ik_y y + ik_z z) | V(x) | R_{nl}(r) Y_l^m(\theta, \varphi) \exp\left\{ (2\pi/3)^{1/2} \gamma [(\xi + k_v) Y_1^1(\theta, \varphi) + (\xi - k_v) Y_1^{-1}(\theta, \varphi)] \right\} \rangle. \end{aligned} \quad (6)$$

Since ξ and k_v are positive constants (of roughly the same magnitude in our experiments), $m = -1$ states will be populated preferentially over $m = 1$ states, producing circular polarization, in agreement with our observation.⁸ This can be arrived at by an intuitive classical argument: For an ion traversing the surface in a $+y$ direction (see Fig. 1) the electron state corresponding to counterclockwise electron orbital motion (which when

these results with Eq. (2), we obtain as a crude estimate $\Delta \approx 0.1$ eV Å; i.e., one to two orders of magnitude smaller than typical values of this quantity obtained for other systems.⁵ This appears reasonable to us only if the initial production of polarization occurs at a distance x_0 that is significantly larger than the turning point, so that the integral in Eq. (3) is greatly reduced. Thus we propose the following picture: The production of orientation occurs as the particle recedes from the surface at distances of at least 2 or 3 Å. This is consistent with our observations that the polarization does not depend upon the initial charge or molecular identity of the projectile and that the sign of the circular polarization is determined by the direction of the outgoing particle as shown in Fig. 2.

In order to identify the physical mechanism that produces orientation, we consider an initially unpolarized ion or atom moving on a straight-line trajectory in the vicinity of a structureless "jellium" surface. This model, although simple, is sufficient to encompass the major electronic processes thought to be operative.⁶ In this model, in order to obtain orientation effects, we must include explicit velocity-dependent interactions. We can do this by attaching a "translational factor" to the electronic wave function of the moving atom to account for the fact that its electrons are moving along with the nucleus.⁷ E.g., for a hydrogen atom,

$$\varphi_H \approx R_{nl}(r) Y_l^m(\theta, \varphi) \exp(-k_v y), \quad (4)$$

where $\hbar k_v$ is the y component of the atom velocity. If we approximate the electronic wave functions of the jellium by

$$\varphi_s \sim \exp(ik_y y + ik_z z - \xi x), \quad (5)$$

the first-order matrix element governing capture of a surface electron by the ion is of the form

close to the surface most closely matches surface electron velocities) will be preferentially populated.

In summary, the following mechanism appears consistent with our observations. As the incident ion approaches the surface at a grazing angle and collides with one or a few atoms on the surface, it experiences a myriad of competing neutraliza-

tion, excitation, de-excitation, and momentum-changing processes. If it is initially a molecule, it may be broken apart. Some anisotropically excited hydrogen atoms may be produced by these essentially ion-atom collisions,⁹ but as the atoms leave the surface, de-excitation and ionization processes rapidly deplete the excited states.⁶ Excited states which survive and ultimately radiate are enriched by those which were formed at relatively large distances from the surface by anisotropic near-resonant electron capture, resulting in nearly pure orientation which is then partially converted to alignment by the surface electrostatic interaction.

¹H. J. Andrä, R. Fröhling, H. J. Plöhn, and J. D. Silver, *Phys. Rev. Lett.* **37**, 1212 (1976).

²H. J. Andrä, R. Fröhling, and H. J. Plöhn, in *Inelastic Ion-Surface Collisions*, edited by N. H. Tolk, J. C. Tully, W. Heiland, and C. W. White (Academic, New

York, 1977), p. 329.

³H. G. Berry, G. Gabrielse, A. E. Livingston, R. M. Schectman, and J. Desesquelles, *Phys. Rev. Lett.* **38**, 1473 (1977).

⁴Y. Band, *Phys. Rev. A* **13**, 2061 (1976), and references therein.

⁵N. H. Tolk, J. C. Tully, J. S. Kraus, C. W. White, and S. Neff, *Phys. Rev. Lett.* **36**, 747 (1976).

⁶H. D. Hagstrum, in *Inelastic Ion-Surface Collisions*, edited by N. H. Tolk, J. C. Tully, W. Heiland, and C. W. White (Academic, New York, 1977), p. 1.

⁷D. R. Bates and R. McCarroll, *Proc. Roy. Soc. London, Ser. A* **245**, 175 (1958).

⁸From Eq. (7), the orientation effects arise because of the presence of the spherical harmonics Y_1^1 and Y_1^{-1} that appear within an exponential. If we were to expand this exponential, keeping only the term linear in the Y 's, we would obtain an approximate selection rule that orientation would be produced only in $l=1$, $m=\pm 1$ states, consistent with our experimental observation that the predominant polarization effects arise from the $3p$ state.

⁹F. J. Eriksen, D. H. Jaecks, W. deRijk, and J. Macek, *Phys. Rev. A* **14**, 119 (1976).

Effect of a dc Electric Field on Beam Trapping

G. J. Morales

Department of Physics, University of California, Los Angeles, California 90024
(Received 13 June 1978)

The role of an external dc electric field on the single-wave trapping dynamics found in the nonlinear evolution of the weak cold-beam-plasma instability is investigated. In the absence of wave damping the beam momentum can be clamped while the wave amplitude increases secularly in time. When damping is present a nonlinear equilibrium is attained in which the beam evolves into a singular charge clump which drifts at constant velocity through the plasma.

It is well known that when a low-density, fast electron beam is injected into a background plasma it triggers an electrostatic two-stream instability. It has been shown both theoretically^{1,2} and experimentally^{3,4} that this instability leads to the growth of a nearly monochromatic electron plasma wave (single mode) whose amplitude saturates by trapping the beam electrons within its potential troughs. The process of beam trapping is of interest to basic plasma physics studies since it provides an example where coherent nonlinear processes play a dominant role, thus entering the domain where the familiar quasilinear theory based on the random-phase approximation is not applicable. On the practical side, saturation by beam trapping limits the maximum energy that can be extracted in traveling-wave tube (TWT)

devices used extensively to generate microwave radiation.

This Letter illustrates the changes produced on the dynamics of beam trapping when an external dc electric field E_0 is applied to the beam particles. This problem is of interest for various reasons: (1) It provides an idealization of the coherent interaction of a population of runaway electrons with collective modes; (2) it explores the possibility of enhancing the efficiency of energy extraction out of beam devices; (3) it simulates the effect of low-frequency turbulence on beam nonlinearities. The major effects found in this study are as follows: (1) The beam can be clamped in energy with the momentum push transferred to the wave; (2) the normal beam saturation level can be significantly enhanced by $E_0 \neq 0$